An Efficient and Safe Trans-complementation System of Mpox Virus Reproduces Authentic Viral Architecture and Infection

Jianying Liu[1,*], Longchao Zhu[1,*], Lingling Mei[1], Yuanyuan Liu[1], Yuanyuan Qu[1], Yulin Yuan[1], Mengjie Zhang[1], Fenfen Zhang[1], Wanbo Tai[1,2], Jun Ma[1], Min Zheng[1], Xiaolu Shi[3], Yang Liu[1,#], Gong Cheng[2,3,#]

1 Institute of Infectious Diseases, Shenzhen Bay Laboratory, Shenzhen 518000, China.
2 New Cornerstone Science Laboratory, Tsinghua University-Peking University Joint Center for Life Sciences, School of Medicine, Tsinghua University, Beijing 100084, China.
3 Institute of Pathogenic Organisms, Shenzhen Center for Disease Control and Prevention, Shenzhen 518055, China.

* These authors contribute equally.
# Corresponding to liuy@szbl.ac.cn, gongcheng@mail.tsinghua.edu.cn.

Abstract

The current Mpox virus (MPXV) outbreak since 2022 has led to 92,783 cases and at least 171 fatalities across 116 countries, with increased transmission noted particularly among male homosexual activities, though the underlying causes remain unknown. The requirement of biosafety level 3 (BSL-3) laboratories poses a barrier to MPXV research and the formulation of antiviral strategies, while genetic modifications to the wild-type live virus raise biosafety and bioethical concerns. Here we report a novel trans-complementary system that produces a single-round infectious MPXV, preserving the virus's authentic architecture and enabling it to complete its life cycle in complementary cells. This deficient MPXV genome lacks two essential genes critical for viral late genes transcription, viral assembly, and release. The entire 197 kb genome of the deficient MPXV was synthesized and assembled *in vitro*, a method that reduces the risk of recombination with bacterial or yeast DNA, in contrast to traditional recombination techniques. The deficient MPXV, limited to single-round infection in various normal cell lines, regained reproductive capability in the complementary cells. Notably, SCID mice inoculated with this deficient MPXV exhibited no detectable disease or viral load in their organs. Therefore, this trans-complementation platform can be safely utilized in BSL-2 laboratories, providing a valuable tool for MPXV research and the development of countermeasures.

Introduction

In the first half of 2022, the Mpox virus (formerly monkeypox virus, MPXV) suddenly emerged in multiple countries and rapidly spread. To date, a total of 92,783 laboratory confirmed cases and 660 probable cases, including 171 deaths, have been reported to WHO from 116 countries[1]. The primary natural hosts of the MPXV are mammals such as rodents, and it mainly spreads through close contact. Symptoms of MPXV range from fever, headache, and rash to severe complications like pneumonia and sepsis, potentially leading to death[2]. The MPXV has two primary genetic evolutionary branches: the West African clade with a 1% fatality rate and the Congo Basin clade with a higher fatality rate of up to 10%[3]. Evidence indicates the 2022 MPXV outbreak is genetically linked to the 2017-2018 Nigerian Mpox epidemic, suggesting it originated from the ongoing evolution of that strain[4]. The MPXV genome, composed of double-stranded DNA, typically evolves at a slow pace. However, the 2022 epidemic strain has surpassed the expected mutation rate, indicating an accelerated evolution of the virus[5]. Other research highlights the current epidemic MPXV's increased adaptability to humans, enhanced transmission capabilities, and altered tissue and organ preferences, particularly evident in the significant transmission among male homosexual populations[6,7]. The underlying causes and molecular mechanisms behind these developments remain unknown.

The MPXV is enveloped, approximately 200-300 nm in diameter, brick-shaped, and features a dumbbell-shaped core[8]. The genome of the MPXV is characterized by a large, double-stranded DNA structure, approximately 197 kilobases in length. The MPXV genome encodes for numerous proteins, involved in various aspects of the virus's life cycle, replication, and interaction with the host's immune system. During the life cycle of the MPXV, two forms of viral particles are present: Intracellular Mature Virus (IMV) and Extracellular Enveloped Virus (EEV). The IMV possesses a single layer of the cellular membrane, whereas the EEV gradually acquires a double-layered phosphatidylethanolamine membrane through a trans-Golgi transport process. Both forms of viral particles are infectious[9]. The Mpox virus infection within cells progresses through early, intermediate, and late stages. Upon entering the cells, both IMV and EEV release prepackaged viral proteins and enzymatic factors into the cytoplasm, stimulating expression of early genes. Early protein synthesis triggers DNA replication, and production of intermediate transcription factors, followed by expression of late genes, mainly structural proteins and enzymes. Eventually, virions assemble from DNA

concatemers with all necessary components for a new infection cycle[10].

Until now, several infectious clone systems of Orthopoxvirus genus have been established, including vaccinia virus (VACV)[11], horsepox virus (HPXV)[12], cowpox virus (CPXV)[13]. The trans-complementation deficient virus system represents a novel viral platform for the studies of high pathogenic viruses under low biosafety conditions[14]. This deficient virus lacks several essential genes necessary for viral replication and propagation, allowing for progeny production of the deficient virus only within specific cell lines that complement these essential genes[14]. To generate the trans-complementation system of MPXV, we selected the G9R and A1L genes on the MPXV, based on the previous research of Orthopoxvirus genus viruses. The G9R gene encodes a late transcription factor VLTF-1, while A1L gene encodes the late transcription factor VLTF-2, both are highly conserved across poxviruses[15]. These two genes have been proven essential for infection and replication within the poxvirus family; loss of either one of them results in the lethality of the poxvirus[16,17]. The absence of these two critical genes, widely separated on the genome, further reduces the risk of viral homologous recombination reverting to the wild type.

In our study, we synthesized 56 Mpox viral genome fragments and assembled them into the complete viral genome *in vitro*, omitting two essential genes, G9R and A1L, and incorporating two fluorescence reporters under the intermediate (G9R) and late (A46R) gene promoters. Supported by fowlpox virus (FWPV), the modified MPXV genome with a hairpin structure was transfected into Vero E6 G9R+A1L complementary cells to rescue the live virus[11]. We assessed the pathogenicity and stability of this deficient MPXV, confirming its safety in various cell types and SCID mice[18]. Notably, the deficient MPXV was shown to elicit standard immune responses and cell death in complementary cell lines, aiding MPXV pathogenesis studies. Additionally, the integrated reporter genes proved useful for antibody neutralization tests and high-throughput drug screening. Our results indicate that this MPXV trans-complementation system is safe for low-biosafety conditions, providing a significant tool for MPXV basic and applied research.

Results

A trans-complementary deficient MPXV system

The trans-complementation system for MPXV produces deficient viral particles capable of only a single round of infection in normal cells[14]. This system includes: (1) viral genomic DNA without the essential G9R and A1L late transcription factors, crucial for viral vitality, and (2) a complementary cell line that continuously expresses the G9R and A1L proteins. The 197 kb MPXV genomic DNA from the MA001 strain was segmented into 56 smaller fragments, synthesized individually. These fragments were then assembled into seven larger fragments and inserted into the pSAMRT plasmid for amplification. Subsequently, these seven fragments were digested using Type II restriction enzymes and ligated to construct the complete MPXV genome *in vitro*. This deficient viral genome omits two essential genes, G9R and A1L, and features a mNeonGreen fluorescence gene at the beginning of the non-essential A46R gene, linked via a 2A linker, alongside a mCherry fluorescence gene under the G9R gene promoter (termed as MPXV G9R+A1L-KO) (Fig. 1a). Successful ligation of the seven large fragments was confirmed by PCR targeting the discontinuous regions between each of these fragments (Fig. 1b). The hairpin structure, essential for Orthopoxviruses, was synthesized and its structure integrity was verified with Mung bean nuclease treatment (Fig. 1c). Hairpins were ligated to both ends of the viral genome to generate a functional genomic DNA construct, as confirmed by Sanger sequencing across the ligation site.

To produce complementary cells, the G9R and A1L genes (linked by IRES) were incorporated into a lentivirus delivery system, which included puromycin or blasticidin for antibiotic selection. The Vero E6 (African green monkey kidney) cells were infected with recombinant lentivirus and after a two-week antibiotic selection, isolated Vero E6 G9R+A1L colonies were analyzed by western blot and immunofluorescence assay (IFA) to verify the expression of G9R and A1L genes (Fig. 1d,e). The Vero E6 G9R+A1L stable cell lines were then pre-infected with FWPV two hours prior to transfection with the deficient MPXV G9R+A1L-KO genome. FWPV facilitated the initiation of early-stage RNA transcription in the deficient MPXV, a process shared among all Orthopoxviruses. Due to species-specific constraints, the FWPV failed to produce infectious viral particles in mammalian cells. Therefore, only the progeny of the deficient MPXV was reproduced after several days of incubation (Fig. 1f). Typically, significant cytopathic effects (CPE) are noticeable 5 to 7 days after transfection (Fig.

1g). The cells are then harvested 10 days post-transfection, at which point significant cell death is observed in about half of the cell population. The deficient MPXV G9R+A1L-KO forms plaques in the Vero E6 G9R+A1L cells normally, comparable to those formed by authentic MPXV (Fig. 1h)[19]. This deficient virus can effectively amplify in the complementary cells (Fig. 1i and Extended Data Fig. 1a), simultaneously generating a green fluorescence signal (Fig. 1j). Then, the deficient viral particles were purified through sucrose density gradient centrifugation and analyzed using western blot with an anti-MPXV A35R polyclonal antibody (Extended Data Fig. 1b). The negative staining of MPXV G9R+A1L-KO particles by a Transmission Electron Microscope confirmed their structural integrity (Fig. 1k). These results demonstrate that the deficient MPXV G9R+A1L-KO maintains the authentic architecture and pathogenic characteristics of the original virus.

The deficient MPXV exhibited sing-round infection in normal cells

The MPXV G9R+A1L-KO virus, lacking two essential genes for viral reproduction, was restricted to single-round infections in normal cells. It regains its reproductive capacity and produces progeny viruses only when infecting cells that fully complemented both G9R and A1L genes (Fig. 2a). To determine the lethality linked to these two genes, the MPXV G9R+A1L-KO was infected in cells partially complementing either the G9R or A1L gene (Fig. 2b). Notably, the double genes knocked out virus failed to replicate in cells complementing only one gene and did not produce any green fluorescence four days post-infection (Fig. 2c,d). Subsequently, 14 cell lines from various species, including animals and humans, and each derived from different tissues, were selected to assess the replication ability of MPXV G9R+A1L-KO. These cell lines were inoculated with a high initial multiplicity of infection (MOI) of 1. Supernatants with cell lysates were collected daily for plaque assays. For the first two days, a small residual of the inoculated virus was detected, but no amplification occurred in any normal cell line from day 3 to day 5 (Fig. 2e). The fluorescence detection clearly showed the absence of green fluorescence in normal cells from day 1 to day 5, while the deficient virus replicated normally in the Vero E6 G9R+A1L complementary cells (Fig. 2f, Extended Data Fig. 2).

The deficient MPXV remains stable throughout serial passages

To validate the genetic stability of these deficient viruses, we performed subculturing

up to 20 passages (P20) on Vero E6 G9R+A1L cells, in three independent replicates. Viruses from P5, P10, P15, and P20 were subjected to PCR analysis to verify the continuous absence of the targeted G9R and A1L genes and the stability of the mNeonGreen fluorescence gene (Extended Data Fig. 3a). All gene deletions and insertions remained stable after 20 passages (Extended Data Fig. 3b). Although the morphology of the plaques appeared slightly larger after 20 passages (Extended Data Fig. 3c), there were no significant green fluorescence changes four days post-infection between P1 and P20 viruses (Extended Data Fig. 3d). Additionally, only one mutation (Δ146999T) affecting protein characteristics were consistently detected across three replicates through full genome sequencing (Extended Data Table 1).

The deficient MPXV was reproducible in various complementary cell lines

The Vero E6 cells are immune-deficient, lacking the capability to produce interferon. Given this, we were interested in whether the MPXV G9R+A1L-KO could amplify in other G9R+A1L complementary cell lines. Using the G9R+A1L lentiviral system, we introduced these two complementary genes into 8 representative cell lines. Following antibiotic selection, we assessed the expression of these two knocked-in genes by western blot. The results confirmed successful expression of the G9R and A1L genes in 8 cell lines, though expression levels varied slightly (Extended Data Fig. 4). Upon inoculating these stable cell lines with MPXV G9R+A1L KO, the virus rapidly amplified in all cell lines (Fig. 2g). However, the viral load varied among the cell lines, with the highest viral load observed in 22RV1 cells, which were derived from human prostate carcinoma epithelial cells (Fig. 2h). This result indicated that the MPXV MA001 strain may have a tissue preference for prostate carcinoma epithelial, correlating with the significant number of male homosexual patients infected with MPXV in this outbreak[6].

Safety evaluation of deficient MPXV virions *in vivo*

To further evaluate the safety of deficient MPXV *in vivo*, we selected the SCID mice, which were susceptible to Orthopoxvirus infection. We inoculated these mice intraperitoneally with a maximum dose of purified MPXV G9R+A1L-KO virions, equivalent to approximately 10^6 PFU/mouse. An initial titer of 2×10^5 PFU/mouse of vaccinia virus (VACV, tiantan strain) was served as the positive control. Clinical symptoms and body weight were monitored, and blood were collected daily for viral load detection. All mice were sacrificed 9 days post-infection to analyze organ viral

loads (Fig. 3a). The results indicated no weight change between the MPXV G9R+A1L-KO and Mock groups, compared to a notable weight loss in VACV-infected mice (Fig. 3b). Additionally, no viremia or clinical symptoms were observed in either the Mock or deficient MPXV groups (Fig. 3c,d). Nine days post-infection, no viral nucleotide residuals were detected in organs from the deficient MPXV group, while significant amounts of VACV were present in all organs (Fig. 3e). Pathological analysis revealed clear damage in the lungs and spleens of VACV-infected mice, but not in those from the deficient MPXV and Mock groups (Fig. 3f). These results demonstrate that deficient MPXV G9R+A1L-KO induces only a single-round infection and lacks virulence in mice.

The deficient MPXV regulates the innate immune response

The deficient MPXV retains the ability to modulate immune responses and activate other cellular signaling pathways, especially the programmed cell death, in complementary cell lines. MPXV G9R+A1L-KO was introduced at an MOI of 0.1 into IFN-α stimulated Hela G9R+A1L cells, with the RNA transcriptome measured at 48 hours post-infection. Results indicated that while IFN-α significantly upregulated interferon-stimulated genes (ISGs), MPXV showed a robust inhibitory effect on ISG expression (Fig. 4a), demonstrating similar transcriptome profiles to those in VACV-infected cells[20]. Meanwhile, like typical Orthopoxvirus infections, inoculation of MPXV G9R+A1L-KO in Hela G9R+A1L cells induced slow but apparent cell death over time, with nearly 20% of cells dying at 48 hours post-infection (Fig. 4b,c). The activation of apoptosis was indicated by the cleavage of caspase 3, 7, and 8 in deficient MPXV-infected cells (Fig. 4d). These results suggest that this trans-complementation system is a valuable platform for studying MPXV pathogenesis *in vitro*.

The anti-MPXV antibodies and drugs evaluation by deficient MPXV

Due to the extensive capacity of the MPXV genome, the deficient MPXV system can accommodate multiple reporters, including fluorescence proteins and luciferase etc. This allows for the establishment of a high-throughput system for screening and evaluating anti-MPXV antibodies and drugs. Firstly, we compared the antibody neutralization capabilities of two previously reported mAbs, 8AH8AI[21] and 7D11[22], against MPXV G9R+A1L-KO and VACV using the $PRNT_{50}$ assay, the gold standard for antibody neutralization tests. These two antibodies neutralized MPXV G9R+A1L-KO as effectively as VACV, demonstrating that viral particles produced by the trans-

complementation system are suitable for assessing antibody efficacy (Fig. 4e,f). Subsequently, we evaluated the potential of the deficient MPXV for high-throughput drug screening (Fig. 4g). MPXV G9R+A1L-KO was pre-mixed with various drugs previously reported to have anti-MPXV capabilities[23-25]. The anti-MPXV IC_{50} values for these compounds were then determined using the classical plaque-forming unit (PFU) assay and a high-throughput green fluorescence cell counting method, respectively. Notably, two drugs, tecovirimat and cidofovir, approved by the U.S. FDA for emergency use against MPXV, displayed potent anti-MPXV efficacy (Fig. 4h,i). The IC_{50} values measured by our trans-complementation system were consistent with those reported in previous studies using authentic live virus[23,24]. Furthermore, we compared the correlation of IC_{50} values derived from the PFU and fluorescence methods, finding that the results from both methods were comparable and correlated well (Fig. 4j, Extended Data Table 2). These findings suggest that this MPXV trans-complementation system is effective for high-throughput, automated screening and evaluation of antibodies and drugs.

Discussion

Our reverse genetic trans-complementation platform for MPXV, along with various complementary cells, offers a powerful tool for *in vitro* studies on MPXV genetic evolution, life cycle, as well as the induced innate immune responses and programmed cell death. The construction of this deficient MPXV can be entirely achieved *in vitro*, offering numerous advantages over traditional recombination and single plaque selection methods[11]. Genetic modifications can be easily introduced into the seven pSMART plasmids, facilitating the assembly of the full-length MPXV genome via ligation. This *in vitro* approch significantly reduces construction time and minimizes the risk of potential recombination between the MPXV genome and bacterial or yeast genomes, compared to the *in vivo* assembly system[12].

The primary advantage of this deficient MPXV system is its enhanced safety. For high-pathogenicity viruses, direct genetic modification of the wild-type virus could potentially enhance pathogenicity, raising biosafety and bioethical concerns. The trans-complementation system introduces an additional safety measure for such reverse genetic engineering. The conditional replication in complementary cells confines the modified pathogens to those specific cells alone, largely reducing risks to operators and the environment. Our results indicate that immune regulation and programmed cell death function normally in complementary cells with deficient MPXV. Moreover, the viral architecture remains authentic, ensuring the system's efficacy for antibody and drug screening while ensuring safety (Fig. 4).

Fowlpox virus was employed to trigger the initiate transcription of the MPXV G9R+A1L-KO DNA genome due to the conservation of polymerases with the Orthopoxvirus genus. Once entry the cells, FWPV releases its RNA polymerase from the core within the virions, which then recognizes and initiates transcription and replication of the deficient MPXV genome. However, due to the absence of specific proteins, FWPV fails to assemble in mammalian cells and hence doesn't produce progeny viruses. This ensures that only pure deficient MPXV particles are assembled and released, obviating the need for single viral plaque selection typical of traditional recombinant genetic modification methods and significantly reducing the time required for viral rescue.

In our trans-complementation system, we integrated two fluorescent proteins into the deficient MPXV genome. The mCherry gene, replacing the absent G9R gene, is regulated by intermediate transcription factors. Meanwhile, the mNeonGreen gene

was fused to the beginning of the late-expressed A46R gene. Consequently, even without complementation of G9R and A1L genes, a high initial MOI infection of deficient MPXV in normal cells can trigger red fluorescence, while green fluorescence appears only in cells where successful complementation occurs. Thus, the red fluorescence can serve as a tool to evaluate viral single-round entry and replication, providing a quick and effective approach for assessments in primary cells lacking complementation.

This trans-complementary system, while reducing safety concerns, still presents few risks due to MPXV's double-stranded DNA nature, which could potentially recombine with the host genome or other spontaneously infected poxviruses. To minimize recombination risks further, the two excised essential genes are broadly separated on the MPXV genome, and the complementary genes are codon-optimized. This spacing reduces the chance of reverting to a fully functional wild-type MPXV through a single recombination event. We have developed systems lacking three or more essential genes; however, they tend to show reduced reproductive efficiency. The two-gene knockout system represents a compromise between safety and efficiency. Crucially, our extensive *in vitro* and *in vivo* safety evaluations affirm the adequacy of this two-gene knockout strategy.

Utilizing this trans-complementation deficient MPXV system, we can investigate specific MPXV gene functions by knocking out or modifying them, including introducing single amino-acid mutations to pinpoint those critical for the 2022 MPXV epidemic. Additionally, we can attach fluorescence proteins to various non-essential MPXV genes to label different regions of the viral particle, such as the extra-membrane, intra-membrane, and core. This allows for precise tracking via single-particle microscopy to monitor the complete process of cell attachment and entry. Furthermore, we can generate various custom-engineered viral tools specifically designed for anti-MPXV antibody and drug screening and evaluation in various scenarios. Overall, our study offers a comprehensive platform for studying MPXV infection, deciphering disease pathogenesis, and developing countermeasures in low-safety conditions.

Methods

Animals and cells

CB17-SCID female mice were purchased from Syagen Biotechnology company (Suzhou, China). Vero E6 (CL-0491), Caco-2 (CL-0050), 22RV1 (CL-0004), RK-13 (CL-0501), LLC-MK2 (CL-0141), SW-13 (CL-0451A), DU 145 (CL-0075), A549 (CL-0016), 293T (CL-0005), Hela (CL-0101), OVCAR-3 (CL-0178), JEG-3 (CL-0127), HCT-8 (CL-0098), HTR-8 (CL-0765) cells were purchased from Procell (Wuhan, China) and cultured in high-glucose Dulbecco's modified Eagle's medium (DMEM, C11965500BT, Gibco) supplemented with 2 mM L-glutamine, 100 U/mL Penicillin-Streptomycin (P/S, 15140122, Gibco), and 10% fetal bovine serum (FBS; HyClone Laboratories, UT). For G9R+A1L complementary cell lines, the following concentrations of puromycin (ant-pr-1, InvivoGen) or blasticidin (ant-bl-1, InvivoGen) were supplemented respectively: Vero E6 G9R+A1L (puromycin, 1:500), RK13 G9R+A1L (puromycin, 1:4000), 22RV1 G9R+A1L (puromycin, 1:2000), Caco-2 G9R+A1L (puromycin, 1:1000), OVCAR-3 G9R+A1L (puromycin, 1:2000), A549 G9R+A1L (blasticidin, 1:100), DU 145 G9R+A1L (puromycin, 1:5000), 293T G9R+A1L (blasticidin, 1:200), and Hela G9R+A1L (blasticidin, 1:2000). All other culture media and supplements were purchased from ThermoFisher Scientific. All cell lines were authenticated using STR methods and tested negative for mycoplasma.

Construction of the MPXV deficient infectious clone

For the construction of the deficient MPXV G9R+A1L-KO infectious virus, 56 DNA fragments covering the full-length MPXV genome (MA001 strain) were synthesized by Qingke company. The deletions of the G9R and A1L genes, along with the insertion of fluorescent proteins, were introduced into the respective regions of genome (Fig. 1a). To generate the F1 to F7 sub-genomic fragments, seven to eight small DNA fragments were assembled the pSMART-BAC 2.0 (42030, Lucigen) plasmid backbone using Gibson Assembly (E2621L, NEB). These recombinant plasmids were then introduced into BAC-Optimized Replicator v2.0 electrocompetent cells (60210, Lucigen) via electroporation at 2500V, 25μF, 300Ω using the Bio-Rad GenePluser Xcell Total system (1652660, Bio-Rad). To construct the full-length MPXV G9R+A1L KO genome, the F1 to F7 plasmids were digested with the PaqCI enzyme (R0745L, NEB) and assembled *in vitro* using T4 ligase (M0202M, NEB) along with hairpins at both ends. Successful ligations were verified through PCR across the ligation sites and DNA

sequencing. The ligation products were then introduced into Vero E6 G9R+A1L complementary cells to rescue the virus. The primers used for MPXV construction was listed in Extended Data Table 3.

Selection of G9R+A1L complementary cell lines

To construct cell lines expressing the MPXV G9R+A1L proteins, the Flag-G9R and HA-A1L genes were synthesized and optimized for mammalian codon expression. For packaging the lentivirus, the pLVX-G9R+A1L-puromycin or pLVX-G9R+A1L-blasticidin plasmids were transfected into 293T cells using the Lenti-X Packaging Single Shots kit (631275, TaKaRa). Lentiviral supernatants were harvested 48 hours post-transfection and filtered through a 0.45 μm membrane (SLHV033RB, Millipore, Burlington, MA). One day before transduction, target cells were seeded in a 6-well plate with DMEM containing 10% FBS. After 12-18 hours, cells were transduced with 0.5 mL of lentivirus for 24 hours in the presence of 12 μg/mL of polybrene (107689, Sigma-Aldrich, St. Louis, MO). Twenty-four hours after transduction, cells from a single well were distributed into four 10-cm dishes and cultured in medium supplemented with the designated concentration of puromycin or blasticidin. The medium containing antibiotics was refreshed every 2 days. After 2-3 weeks of selection, visible puromycin or blasticidin-resistant cell colonies were formed. Select colonies were moved into 24-well plates. Upon reaching confluence, cells were treated with trypsin and replated in 6-well plates for further growth. These cells were designated as P0 cells. For cell line validation, total cellular mRNA was extracted, subjected to RT-PCR, followed by cDNA sequencing of the G9R and A1L genes, and protein expression was verified via western blot.

Rescue of the deficient MPXV G9R+A1L-KO infectious virus

The deficient MPXV G9R+A1L-KO infectious virus was recovered in the Vero E6 G9R+A1L cell line, which constitutively expresses G9R and A1L proteins. In brief, confluent monolayers of the Vero E6 G9R+A1L cell line in 12-well plates were infected with 1 MOI of avian pox virus (Quail adapted strain, CVCC AV1003) for 2 hours prior to MPXV DNA transfection. Subsequently, the culture media were replaced with Opti-MEM (31985062, Gibco), and DNA transfection was performed using Fugene 6 reagent (E2691, Promega). 1 μg of MPXV DNA was mixed with 3 μl of Fugene 6 reagentin 100 μl Opti-MEM medium for 15 minutes at room temperature. The DNA mix was then slowly dripped onto the cells and gently mixed. Post 24-hour incubation, the

cell supernatant was replaced with fresh 2% FBS DMEM for continued cultivation. Cell monitoring continued for 8-10 days until the appearance of cytopathic effects (CPE) and expression of mCherry and mNeonGreen fluorescent proteins. The supernatant and cells underwent 2 freezing and thawing cycles at −80 °C. After centrifugation at 1000 g for 10 minutes, the supernatants were aliquoted and stored at −80 °C as the P0 virus stock.

Virus plaque assay

10-fold dilutions of the deficient MPXV virus stock were prepared in a 96-well plate in triplicate. The diluted MPXV viruses were added to the Vero E6 G9R+A1L cells for a 2-hour incubation. Cells were then washed thrice with DPBS to eliminate any unattached virus particles. 3 mL of overlay medium (2% FBS DMEM with 2% HEPES, 1% penicillin/streptomycin, and 0.8% carboxymethyl cellulose) was added over the cells for a 6-day incubation. Subsequently, cells were fixed with 4% formaldehyde for 1 hour and stained with 300 μL of 0.5% crystal violet solution for 5 minutes. Plaques were manually counted under whiteboard illumination.

Virus replication kinetics determination

Virus replication kinetics were determined by using a plaque assay as described above. Typically, cell lines were seeded in 24-well plates and cultured at 37 °C with 5% CO_2 for 16 hours. Deficient MPXV was then inoculated into the cells at the specified MOI and incubated at 37 °C for 2 hours. Post-infection, cells were washed thrice with DPBS to eliminate any unattached virus particles. At designated time points, supernatants and cells were collected and underwent 2 freezing and thawing cycles. Following centrifugation at 1000 g for 5 minutes, the supernatants were employed to determine virus titers via plaque assay.

Safety evaluation of deficient MPXV in mice model

Three-to-four-week-old female CB17-SCID mice were randomly assigned and intraperitoneally inoculated with 1×10^6 PFU of MPXV-G9R-A1L-KO, 2×10^5 PFU of VACV, or PBS mock control. Throughout the study, the mice were monitored daily for clinical signs. Blood samples were taken daily for viral DNA extraction to detect the presence of the virus. At 10 d.p.i., the mice were euthanized, and tissue samples were collected for hematoxylin and eosin (H&E) staining and virus titration. All samples were then stored at −80 °C until analysis.

Real-time qPCR assay

Deficient MPXV was isolated using the EZNA SE Viral DNA/RNA kit (R6871, Omega) according to the manufacturer's instructions. The absolute copy number of MPXV DNA was quantified using the 2×EasyTaq® PCR SuperMix (AS111-01, TransGene) by Taqman qPCR. The detection probe and primers were based on the conserved DNA polymerase (F8L) gene and described as follows: Forward primer (5'-TCA ACT GAA AAG GCC ATC TAT G-3'), Reverse primer (5'-GAG TAT AGA GCA CTA TTT CTA AAT CCC A-3'), and probe 5'-FAM-CCA TGC AAT A(T–BHQ1) A CGT ACA AGA TAGTAG CCA AC-Phos-3', both were synthesized by Qingke company. The qPCR reactions were performed using the CFX96 real-time PCR detection system (1855195, Bio-Rad).

Immunofluorescence assay and western blot

For immunofluorescence assay (IFA) staining, Vero E6 G9R+A1L cells were cultured on a Nunc™ Lab-Tek™ II Chamber Slide™ System. G9R and A1L proteins were labeled with primary anti-Flag (F1804, Sigma-Aldrich) and anti-HA (26183, Invitrogen), followed by secondary Alexa Fluor 488 anti-mouse HRP antibody (A28175, Invitrogen). The nuclei were then stained with DAPI. Fluorescence signals were captured using a Nikon fluorescence microscope. For western blot analysis, various types of cells transduced with G9R, A1L, G9R+A1L, or those infected with deficient MPXV were harvested and lysed using RIPA buffer. They were then probed with anti-Flag, anti-HA, and anti-MPXV A35R (RVV13101, AtaGenix) antibodies. The results were analyzed using ImageLab software version 6.0.1 (#12012931, Bio-Rad).

Deficient MPXV antiviral drug evaluation

Vero E6 G9R+A1L cells were seeded in 12-well plates at a specified density. Twenty-four hours post-seeding, MPXV G9R+A1L-KO (with a final inoculation of 50 PFU per well) was pre-mixed with varying drug concentrations before adding to the cells. After a 2-hour incubation at 37°C and 5% CO_2 with gentle rocking every 15 minutes, the inoculum was removed. Cells were then overlaid with a mixture of 2% HEPES, 1% penicillin/streptomycin, and 0.8% carboxymethyl cellulose (C104979, Aladdin) in DMEM, with each condition tested in triplicate. Plates were then incubated for 6 to 8 days at 37°C in a 5% CO_2 incubator. Monolayers were fixed in 4% formaldehyde and stained with 0.5% crystal violet. Plaques were manually counted under whiteboard illumination. IC_{50} values were calculated using GraphPad Prism 9.

Deficient MPXV neutralization assay

The neutralizing activity of monoclonal antibodies (mAbs) was determined using the EEV or IMV forms of VACV, or MPXV G9R+A1L-KO in a plaque reduction neutralization (PRNT) assay. Briefly, 100 PFU of either VACV or deficient MPXV were incubated with serial two-fold dilutions of the mAb for 30 minutes at 37°C and then added to monolayers of Vero E6 or Vero E6 G9R+A1L cells in 6-well plates. After a one-hour incubation, cells were overlaid with 0.8% carboxymethyl cellulose in DMEM with 2% FBS and incubated for 3 days (for VACV) or 6 days (for MPXV G9R+A1L-KO) at 37°C in 5% CO_2 to allow plaque formation. Monolayers were then fixed with 4% formaldehyde and stained with 0.5% crystal violet. Plaques were manually counted under whiteboard illumination.

Statistics

Mice were randomly allocated into different groups. The investigators were not blinded to allocation during the experiments or to the outcome assessment. No statistical methods were used to predetermine sample size. Descriptive statistics are provided in the figure legends. A linear regression model in the software Prism 9 (GraphPad) was used to calculate the IC_{50} values from the antiviral assay. Differences between continuous variables were assessed using the non-parametric Mann-Whitney test. The weight loss data are presented as mean ± standard deviation and were statistically analyzed using two-factor analysis of variance (ANOVA) with Tukey's post hoc test. *, $p < 0.05$; **, $p < 0.01$; ***, $p < 0.001$; ****, $p < 0.0001$; ns, $p > 0.05$, not significant.

Data availability

Extended Data includes 4 figures, and 3 tables can be found with this article. Any other information is available upon request.

Acknowledgments

This study was supported by grants from the National Key Research and Development Plan of China (2021YFC2300200, 2021YFC2302405, 2022YFC2303200, 2022YFC2303400, 2023YFC2307400, and 2023YFC2305900), the National Natural Science Foundation of China (82241082, 32270182, 82372254, 32188101, 31825001, 32273099 and 81961160737), the Research Fund-Vanke School of Public Health, Tsinghua University (2023JC002), Shenzhen Science and Technology Project (JSGG20191129144225464), Shenzhen Medical Research Fund (B2301009),

475 Shenzhen San-Ming Project for Prevention and Research on Vector-borne Diseases
476 (SZSM202211023), Innovation Team Project of Yunnan Science and Technology
477 Department (202105AE160020). The New Cornerstone Science Foundation through
478 the New Cornerstone Investigator Program, and the Xplorer Prize from Tencent
479 Foundation.

480 **Author contributions**

481 G.C. and Y.L. conceived and designed the study. G.C., Y.L., J.L. and L.Z. wrote and
482 revised the manuscript. J.L., L.Z., L.M., Y.L., Y.Q., Y.Y., M.Z., F.Z., W.T., J.M., M.Z., and
483 Y.L. performed the experiments and analyzed the data. X.S. provided critical reagents.
484 All the authors reviewed, critiqued, and provided comments on the text.

485 **Competing financial interests**

486 The authors declare no competing interests.

References

1. WHO. 2022 Monkeypox Outbreak: Global Trends. https://worldhealthorg.shinyapps.io/mpx_global/

2. Gong Q, Wang C, Chuai X, Chiu S. Monkeypox virus: a re-emergent threat to humans. *Virol Sin* 2022, 37(4): 477-482.

3. Adnan N, Haq ZU, Malik A, Mehmood A, Ishaq U, Faraz M, et al. Human monkeypox virus: An updated review. *Medicine (Baltimore)* 2022, 101(35): e30406.

4. Yinka-Ogunleye A, Aruna O, Dalhat M, Ogoina D, McCollum A, Disu Y, et al. Outbreak of human monkeypox in Nigeria in 2017-18: a clinical and epidemiological report. *Lancet Infect Dis* 2019, 19(8): 872-879.

5. Isidro J, Borges V, Pinto M, Sobral D, Santos JD, Nunes A, et al. Phylogenomic characterization and signs of microevolution in the 2022 multi-country outbreak of monkeypox virus. *Nat Med* 2022, 28(8): 1569-1572.

6. Endo A, Murayama H, Abbott S, Ratnayake R, Pearson CAB, Edmunds WJ, et al. Heavy-tailed sexual contact networks and monkeypox epidemiology in the global outbreak, 2022. *Science* 2022, 378(6615): 90-94.

7. O'Toole A, Neher RA, Ndodo N, Borges V, Gannon B, Gomes JP, et al. APOBEC3 deaminase editing in mpox virus as evidence for sustained human transmission since at least 2016. *Science* 2023, 382(6670): 595-600.

8. Cho CT, Wenner HA. Monkeypox virus. *Bacteriol Rev* 1973, 37(1): 1-18.

9. Schmelz M, Sodeik B, Ericsson M, Wolffe EJ, Shida H, Hiller G, et al. Assembly of vaccinia virus: the second wrapping cisterna is derived from the trans Golgi network. *J Virol* 1994, 68(1): 130-147.

10. Rubins KH, Hensley LE, Bell GW, Wang C, Lefkowitz EJ, Brown PO, et al. Comparative analysis of viral gene expression programs during poxvirus infection: a transcriptional map of the vaccinia and monkeypox genomes. *PLoS One* 2008, 3(7): e2628.

11. Yoshikawa T, Fujii H, Okutani A, Shibamura M, Omura N, Egawa K, et al. Construction and characterization of bacterial artificial chromosomes harboring the full-length genome of a highly attenuated vaccinia virus LC16m8. *PLoS One* 2018, 13(2): e0192725.

12. Noyce RS, Lederman S, Evans DH. Construction of an infectious horsepox virus vaccine from chemically synthesized DNA fragments. *PLoS One* 2018, 13(1): e0188453.

13. Roth SJ, Hoper D, Beer M, Feineis S, Tischer BK, Osterrieder N. Recovery of infectious virus from full-length cowpox virus (CPXV) DNA cloned as a bacterial artificial chromosome (BAC). *Vet Res* 2011, 42(1): 3.

14. Zhang X, Liu Y, Liu J, Bailey AL, Plante KS, Plante JA, et al. A trans-complementation system for SARS-CoV-2 recapitulates authentic viral replication without virulence. *Cell* 2021, 184(8): 2229-2238. e2213.

15. Upton, C., et al., Poxvirus orthologous clusters: toward defining the minimum essential poxvirus genome. *J Virol* 2003. 77(13): p. 7590-600.

16. Zhang Y, Keck JG, Moss B. Transcription of viral late genes is dependent on expression of the viral intermediate gene G8R in cells infected with an inducible conditional-lethal mutant vaccinia virus. *J Virol* 1992, 66(11): 6470-6479.

17. Dobson, B.M. and D.C. Tscharke, Redundancy complicates the definition of essential genes for vaccinia virus. *J Gen Virol* 2015. 96(11): p. 3326-3337.

18. Futami, M., et al., Efficacy and Safety of Doubly-Regulated Vaccinia Virus in a Mouse Xenograft Model of Multiple Myeloma. *Mol Ther Oncolytics* 2017. 6: p. 57-68.

19. Huang B, Zhao H, Song J, Zhao L, Deng Y, Wang W, et al. Isolation and Characterization of Monkeypox Virus from the First Case of Monkeypox - Chongqing Municipality, China, 2022. *China CDC Wkly* 2022, 4(46): 1019-1024.

20. Hernaez, B., et al., RNA-Seq Based Transcriptome Analysis of the Type I Interferon Host Response upon Vaccinia Virus Infection of Mouse Cells. *J Immunol Res* 2017. 2017: p. 5157626.

21. Chen, Z., et al., Chimpanzee/human mAbs to vaccinia virus B5 protein neutralize vaccinia and smallpox viruses and protect mice against vaccinia virus. *Proc Natl Acad Sci U S A* 2006. 103(6): p. 1882-7.

22. Esqueda, A., et al., A Monoclonal Antibody Produced in Glycoengineered Plants Potently Neutralizes Monkeypox Virus. *Vaccines (Basel)* 2023. 11(7).

23. Warner, B.M., et al., In vitro and in vivo efficacy of tecovirimat against a recently emerged 2022 monkeypox virus isolate. *Sci Transl Med* 2022. 14(673): p. eade7646.

24. Frenois-Veyrat G, Gallardo F, Gorge O, Marcheteau E, Ferraris O, Baidaliuk A, et al. Tecovirimat is effective against human monkeypox virus in vitro at nanomolar concentrations. *Nat Microbiol* 2022, 7(12): 1951-1955.

25. Chiem, K., et al., Identification of In Vitro Inhibitors of Monkeypox Replication. *Microbiol Spectr* 2023. 11(4): p. e0474522.

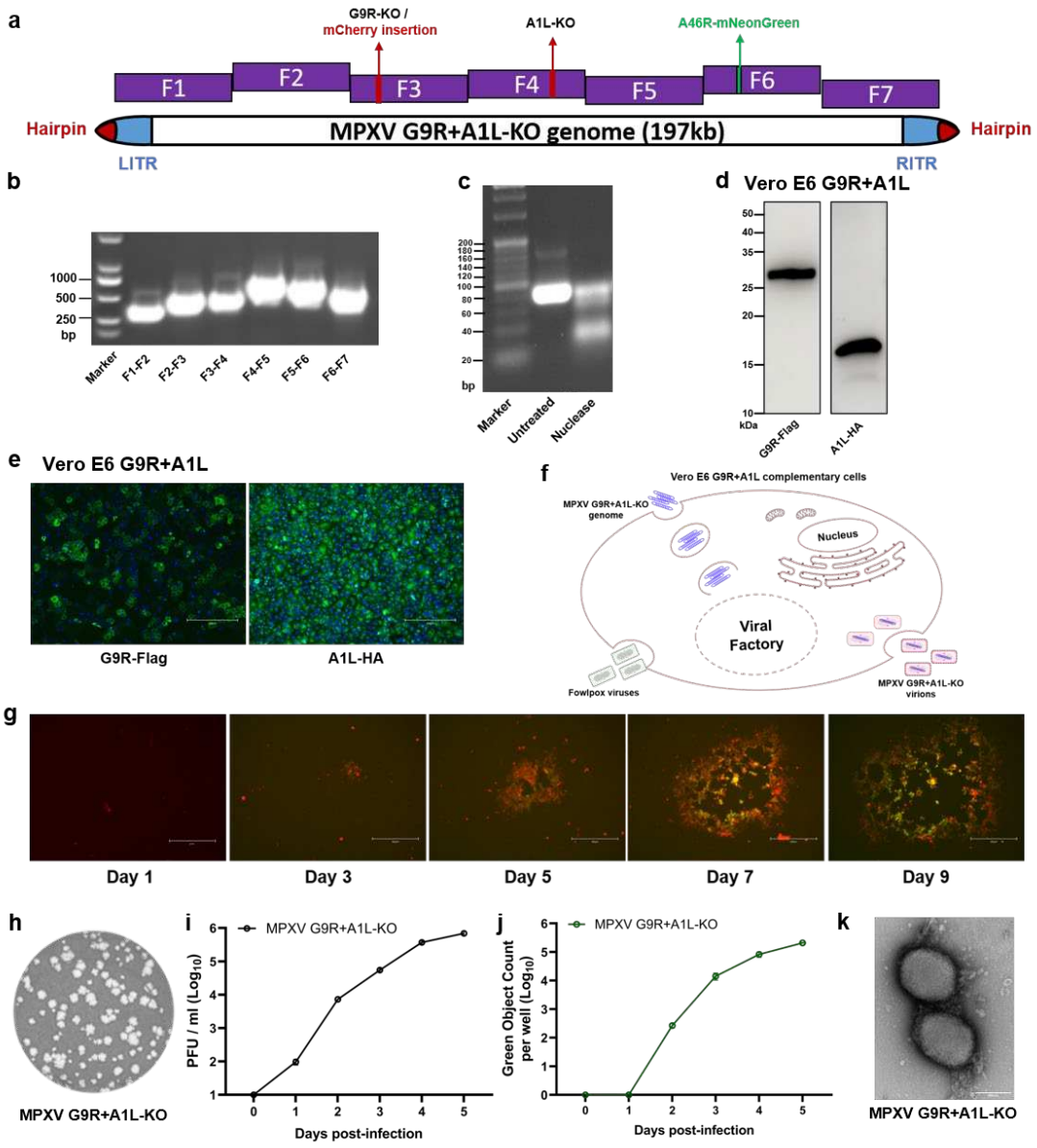

Figure 1

Figure 1. Construction and rescue of trans-complementation deficient Mpox virus.

a, Schematic representation of deficient MPXV G9R+A1L-KO construction. Deletions of the G9R and A1L genes, along with the insertion of fluorescent proteins, were introduced into the backbone of MPXV MA001 strain. The complete MPXV genome was assembled from seven big fragments. Red arrows highlight the loci of G9R and A1L gene knockouts on the MPXV genome, with an mCherry reporter inserted at the G9R site. The green arrow marks the insertion site of the mNeonGreen reporter. **b,** Validation the integrity of full-length MPXV genome by PCR. Primers spanning fragment junctions were employed to verify the complete assembly of the MPXV genome. **c,** Validation of the secondary structure formation of synthesized MPXV hairpin oligos. The Mung bean exo/endonuclease recognized and digested double strand DNAs. **d,e,** The expression and localization of G9R and A1L genes in Vero E6

570 G9R+A1L complementary cells were detected by western blot **(d)**, and
571 immunofluorescence assay **(e)**; Scale bar, 300 μm. **f,** The diagram for rescue of
572 deficient MPXV infectious clone. The Vero E6 G9R+A1L stable cell lines were pre-
573 infected with FWPV two hours prior to transfection with the deficient MPXV G9R+A1L-
574 KO genome. FWPV facilitated the initiation of early-stage RNA transcription in the
575 deficient MPXV. Due to species-specific constraints, the FWPV failed to produce
576 infectious viral particles in mammalian cells. Therefore, only the progeny of the
577 deficient MPXV was reproduced after several days of incubation. **g,** Observation of
578 time-lapse MPXV G9R+A1L-KO viral plaque formation using mCherry and
579 mNeonGreen fluorescence detection; Scale bar, 300 μm. **h,** Plaque morphology of
580 MPXV G9R+A1L-KO virus in Vero E6 G9R+A1L complementary cells. The plaques
581 were stained using crystal violet 6 days post-infection. **i,j,** Replication kinetics of MPXV
582 G9R+A1L-KO virus in Vero E6 G9R+A1L complementary cells. 0.01 MOI of MPXV
583 G9R+A1L-KO virus was inoculated onto Vero E6 G9R+A1L cells. Following a 2-hour
584 incubation, the cells were washed three times with DPBS and continuously cultured
585 for 5 days with fresh 2% FBS DMEM. The virus titers and mNG-positive cells were
586 determined using a plaque assay (**i**) and fluorescence determination (**j**). **k,** Electron
587 microscopy of MPXV G9R+A1L-KO virus particles with negative staining; Scale bar,
588 200 nm.
589

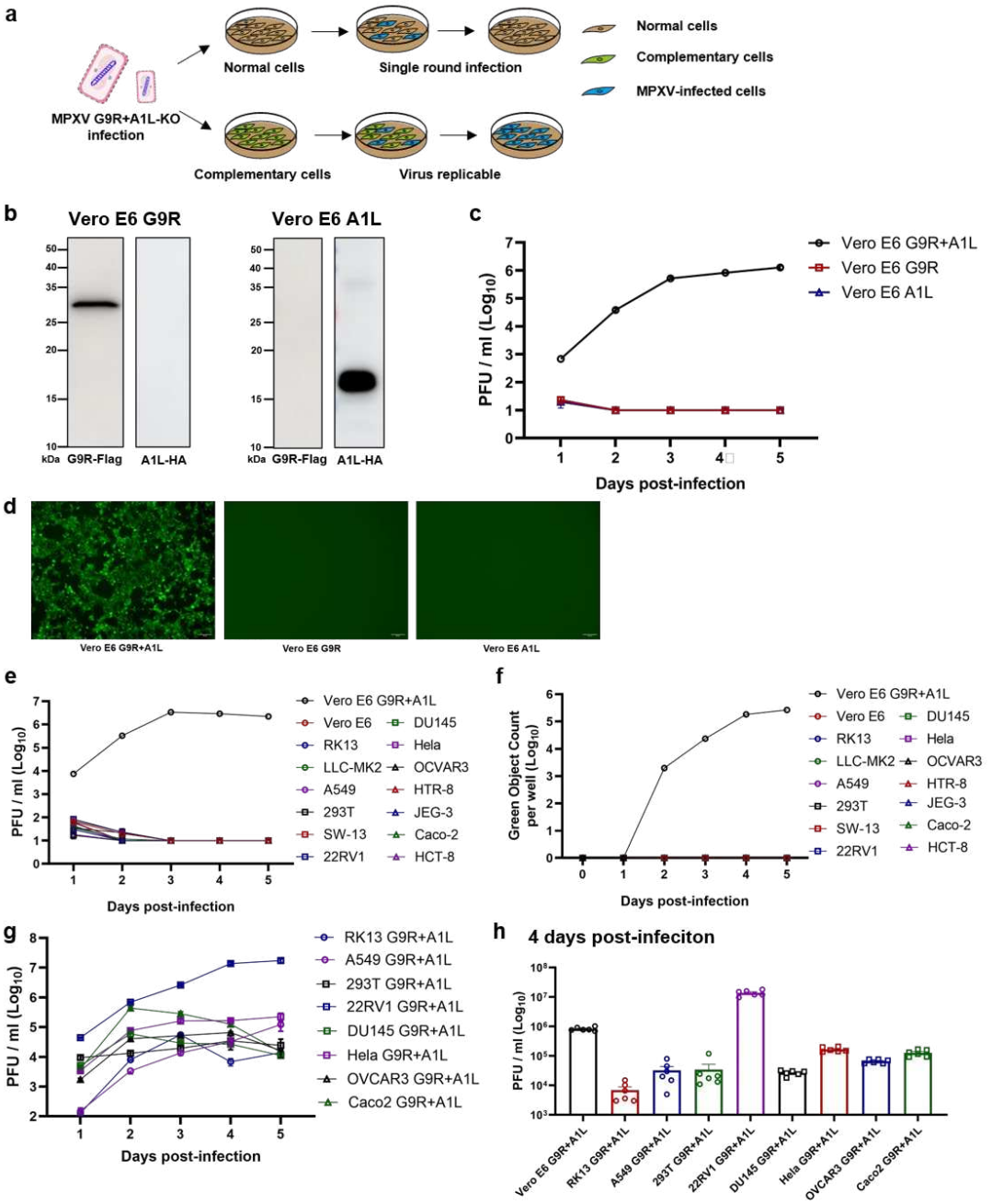

Figure 2

Figure 2. Replication dynamics of MPXV G9R+A1L-KO virion in normal and complementary cells.

a, Schematic representation of the replication of MPXV G9R+A1L-KO virion in both normal and complementary cells. **b,** The expression of G9R and A1L genes in Vero E6 G9R and Vero E6 A1L partially complementary cells respectively. **c,** Replication kinetics of the MPXV G9R+A1L-KO virus in Vero E6 G9R+A1L, Vero E6 G9R, and Vero E6 A1L complementary cells. Each cell type was inoculated with 0.1 MOI of the MPXV G9R+A1L-KO virus. The virus titers were determined using a plaque assay. **d,** Fluorescence microscopy analysis of deficient MPXV infected complementary cell lines. Representative mNeonGreen (mNG) positive images at 4 days post infection are

shown. Scale bar, 100 μm. **e,f,** Assessment of single-round infection of MPXV G9R+A1L-KO virus on normal cell lines. 1 MOI of MPXV G9R+A1L-KO virus was inoculated onto 14 different cell lines. The Vero E6 G9R+A1L cell served as positive control. The virus titers and mNG-positive cells were determined using a plaque assay (**e**) and fluorescence determination (**f**). **g,** Replication kinetics of MPXV G9R+A1L-KO virus in different G9R+A1L complementary cells. 0.1 MOI of MPXV G9R+A1L-KO virus was inoculated onto eight G9R+A1L complementary cells. The virus titers were determined using a plaque assay. **h,** The virus titers of G9R+A1L complementary cells at 4 days post-infection with MPXV G9R+A1L-KO virus are presented side by side for comparison.

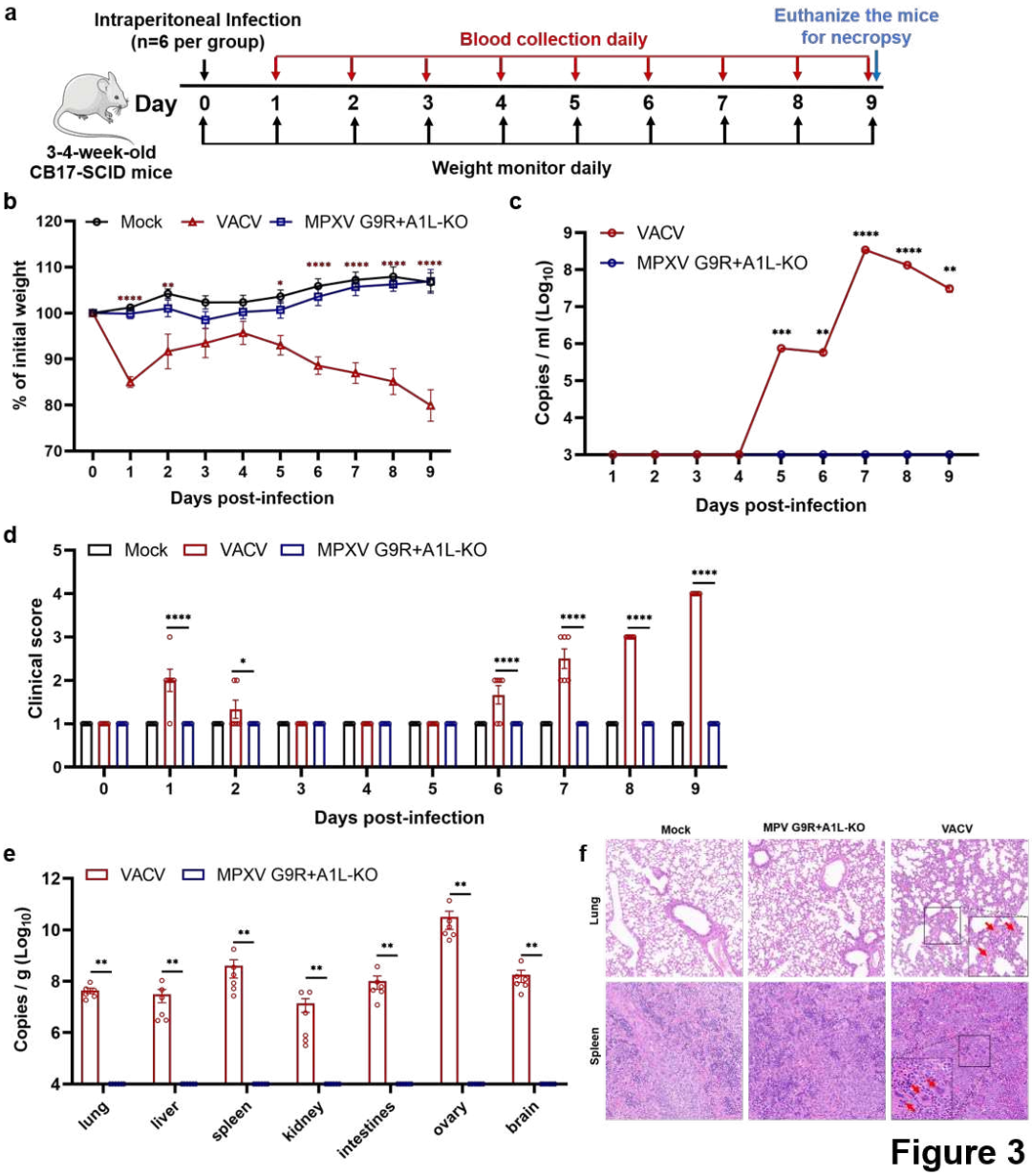

Figure 3

Figure 3. The safety evaluation of MPXV G9R+A1L-KO virion in animal models. **a,** Experimental scheme of MPXV G9R+A1L-KO virus challenge. 3-4 weeks old SCID mice were intraperitoneally (I.P.) inoculated with 1×10^6 PFU of MPXV G9R+A1L-KO virus, 2×10^5 PFU of VACV, or PBS mock control, respectively. Mice were monitored for weight loss, disease, and viral load. **b,** The weight changes of animals after intraperitoneal infection of MPXV G9R+A1L-KO virus (n=6) and VACV (n=6). The uninfected mock group (n=6) served as a negative control. Body weights were recorded daily for 9 days. Data are presented as mean ± standard deviation. Weight changes between MPXV G9R+A1L-KO and mock or VACV groups were assessed using two-way ANOVA with Tukey's post hoc test. The red asterisk indicates a statistical difference between the mock and VACV groups. No significant difference was observed between mock and MPXV G9R+A1L-KO groups. **c,** Viral replication kinetics in serum of infected animals. The amounts of genomic DNA were quantified

by quantitative PCR. **d,** Disease of MPXV G9R+A1L-KO and VACV-infected animals. The diseases include ruffled fur, lethargic, hunched posture, and orbital tightening. The clinical scores are presented. P values were adjusted using the Bonferroni correction to account for multiple comparisons. **e,** The viral loads in lung, liver, spleen, kidney, intestines, ovary and brain after infection with G9R+A1L-KO virus and VACV. Dots represent individual animals (n=6). **f,** Pathological observations of lung and spleen sections in mice. Representative hematoxylin and eosin (H&E) staining images were presented. **c-e,** The mean ± standard error of mean is presented. A non-parametric two-tailed Mann-Whitney test was used to determine the differences between VACV and MPXV G9R+A1L-KO groups. **b-e,** Differences were considered significant if $p < 0.05$; *, $p < 0.05$; **, $p < 0.01$; ***, $p < 0.001$; ****, $p < 0.0001$.

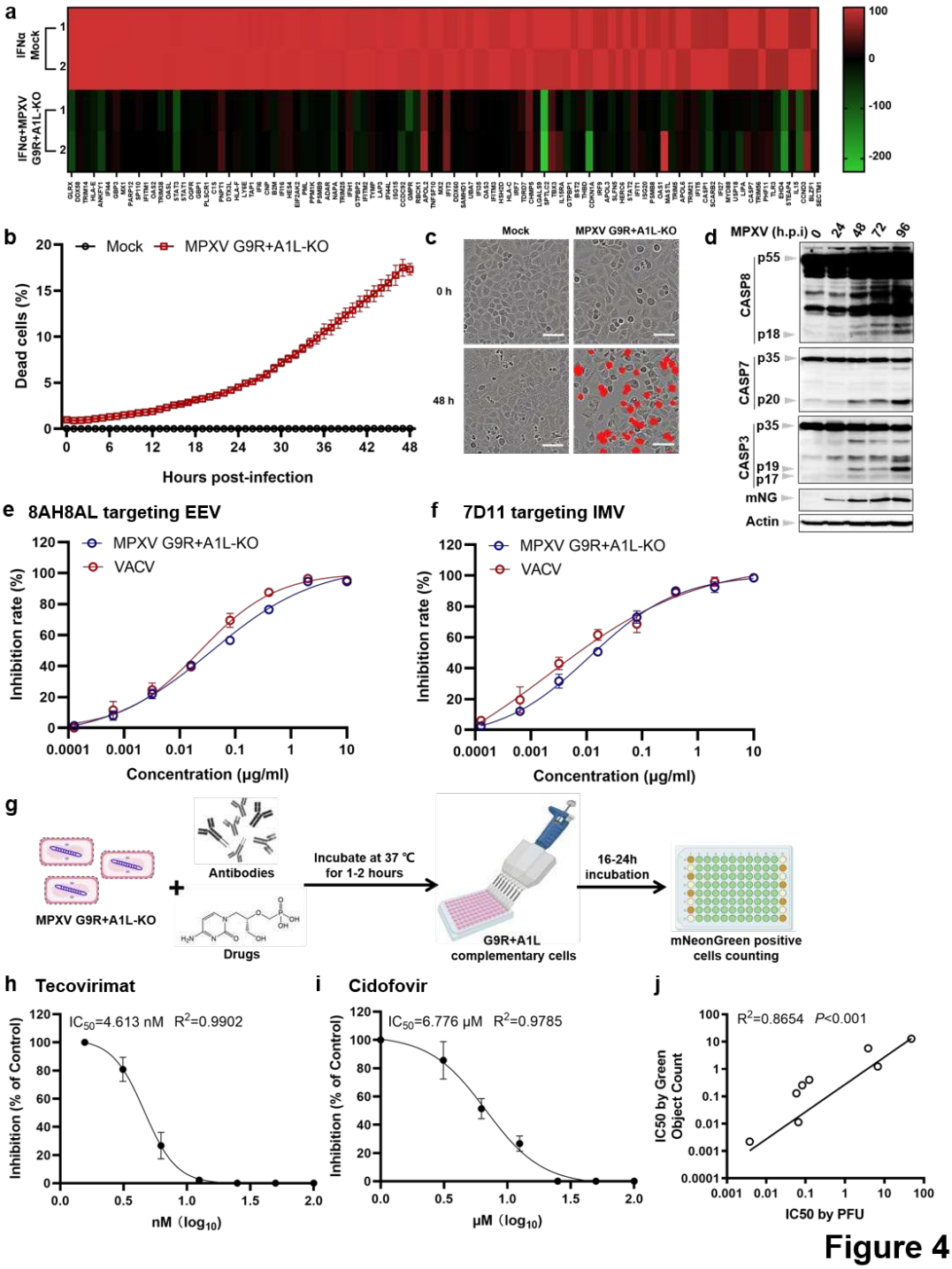

Figure 4

Figure 4. The potential of deficient MPXV for pathogenesis studies, antibody neutralization and high-throughput drug screening.

a, Heatmap of differentially expressed genes (DEGs) associated with IFNα responses in Hela G9R+A1L cells. The heatmap shows the relative percentages of DEGs involved in IFNα responses in deficient MPXV-infected samples versus uninfected cells, with a color scale on the right indicating expression levels. **b-d,** The deficient MPXV stimulates the programmed cell death. **b,** Cell death kinetics were assessed using the IncuCyte live-cell automated system. Hela G9R+A1L cells, seeded in 24-well plates,

were infected with MPXV G9R+A1L-KO virus at an MOI of 0.1. Dead cells, stained with propidium iodide (PI), were counted hourly over a 48-hour period. **c,** PI-positive cells were marked with a red mask for visualization. Scale bar, 80 μm. **d,** The activation of caspase 3, 7, and 8 post-MPXV G9R+A1L-KO infection at different time points. **e,f,** Neutralization activity of monoclonal antibodies (mAbs) against MPXV G9R+A1L-KO and VACV. The 8AH8AL(**e**) and 7D11(**f**) antibodies were incubated with EEV and IMV forms of MPXV G9R+A1L-KO and VACV, respectively, for neutralization via a plaque assay. Curves were fitted using nonlinear regression and mean ± standard deviations from two independent experiments were shown. The experiment was conducted twice with similar results. **g,** Scheme diagram for high-throughput MPXV antibody or drug screening using an mNG positive cell counting assay. **h,i,** The IC_{50} assessment of tecovirimat and cidofovir potency against deficient MPXV in complementary cells. Vero E6 G9R+A1L cells were infected with MPXV G9R+A1L-KO virus and treated with indicated concentrations of tecovirimat (**h**) or cidofovir (**i**) for 6 days. Plaque formation inhibition is expressed in %, normalized over control conditions. IC_{50} and R^2 are indicated. Data are presented as mean ± standard deviations. Experiments were performed twice in triplicate. **j,** Correlation analysis of IC_{50} values between the mNG positive cell counting assay and plaque formation assay. The Pearson correlation coefficient (R^2) and p-values (two-tailed) are indicated.

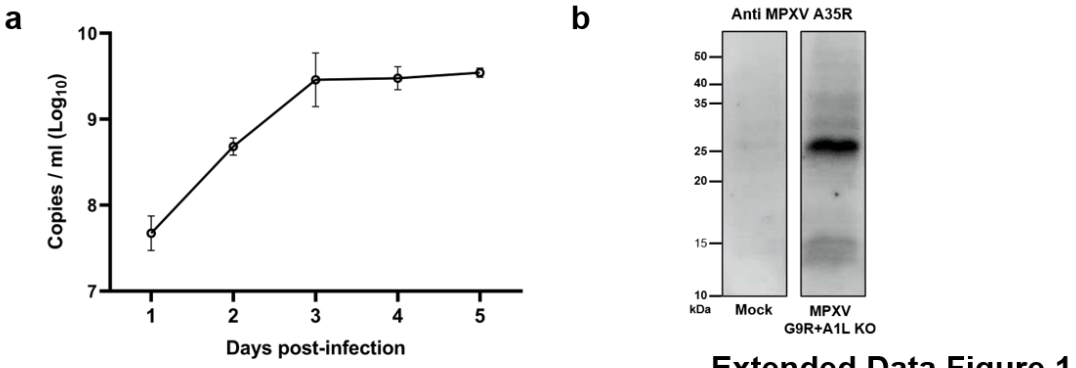

Extended Data Figure 1

664

665 **Extended Data Figure 1. The qPCR and western blot verification of deficient**
666 **MPXV.**

667 **a,** Viral replication kinetics of MPXV G9R+A1L-KO in Vero E6 G9R+A1L cells. The
668 amounts of genomic DNA were quantified by quantitative real-time PCR. **b,** The
669 expression of A35R gene in MPXV G9R+A1L-KO infected or un-infected cell lysates
670 was detected by western blot.

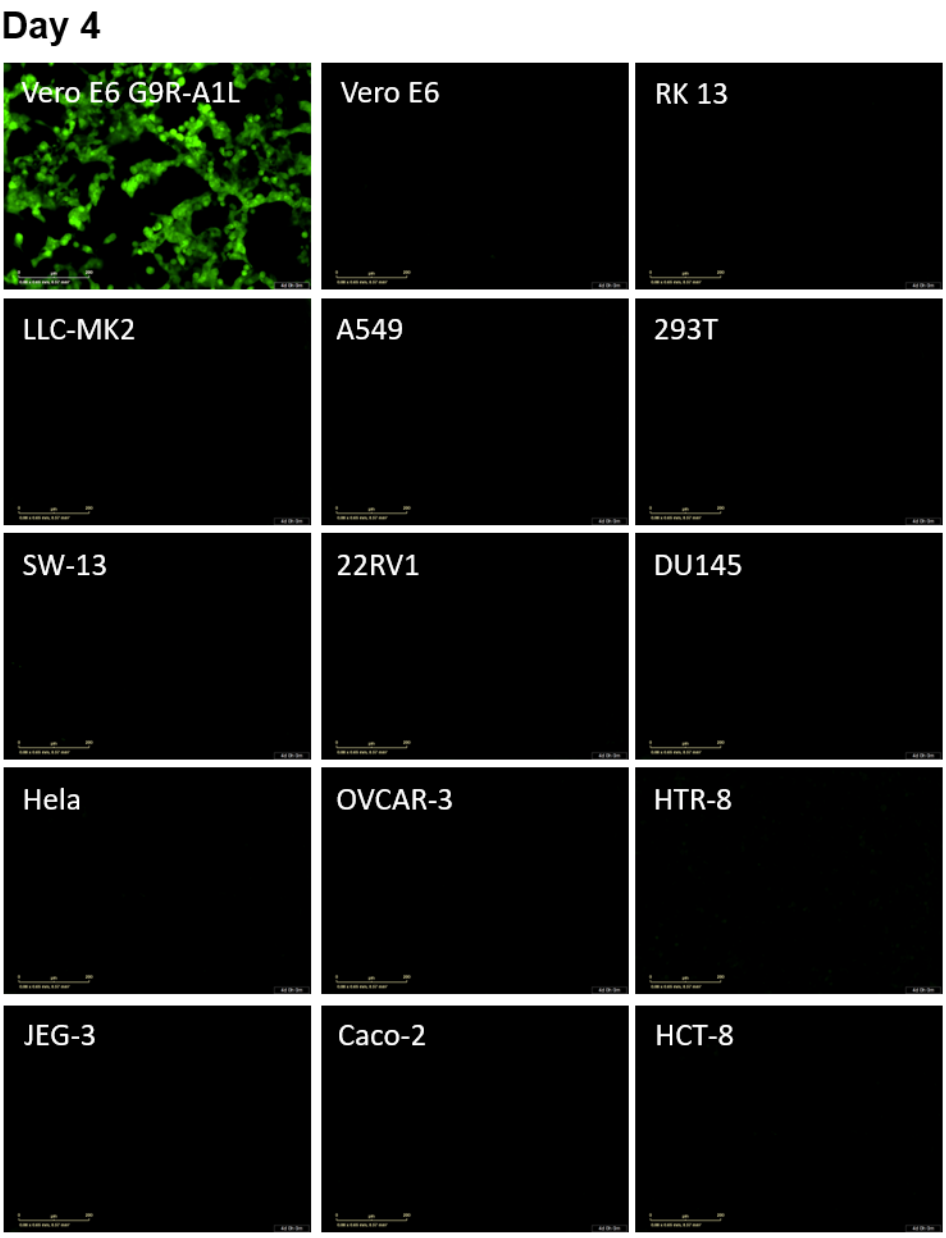

Extended Figure 2. Analysis of deficient MPXV-infected normal and complementary cell lines using fluorescence microscopy.

1 MOI of MPXV G9R+A1L-KO virus was inoculated onto 14 normal cell lines. The Vero E6 G9R+A1L cell was served as a positive control. Representative mNeonGreen positive images at 4 days post infection are shown. Scale bar, 200 μm. Vero E6, African green monkey kidney cells; RK-13, rabbit kidney cells; LLC-MK2, rhesus kidney cells; A549, human non-small cell lung cancer cells; 293T, human embryonic kidney cells; SW-13, human adrenocortical small cell carcinoma cells; 22RV1, human prostate cancer cells; DU 145, human prostate cancer cells; Hela, human cervical cancer cells; OVCAR-3, human ovarian cancer cells; HTR-8, human chorionic trophoblast cells; JEG-3, human chorionic carcinoma cells; Caco-2, human colorectal adenocarcinoma cells; HCT-8, human ileocecal cancer cells.

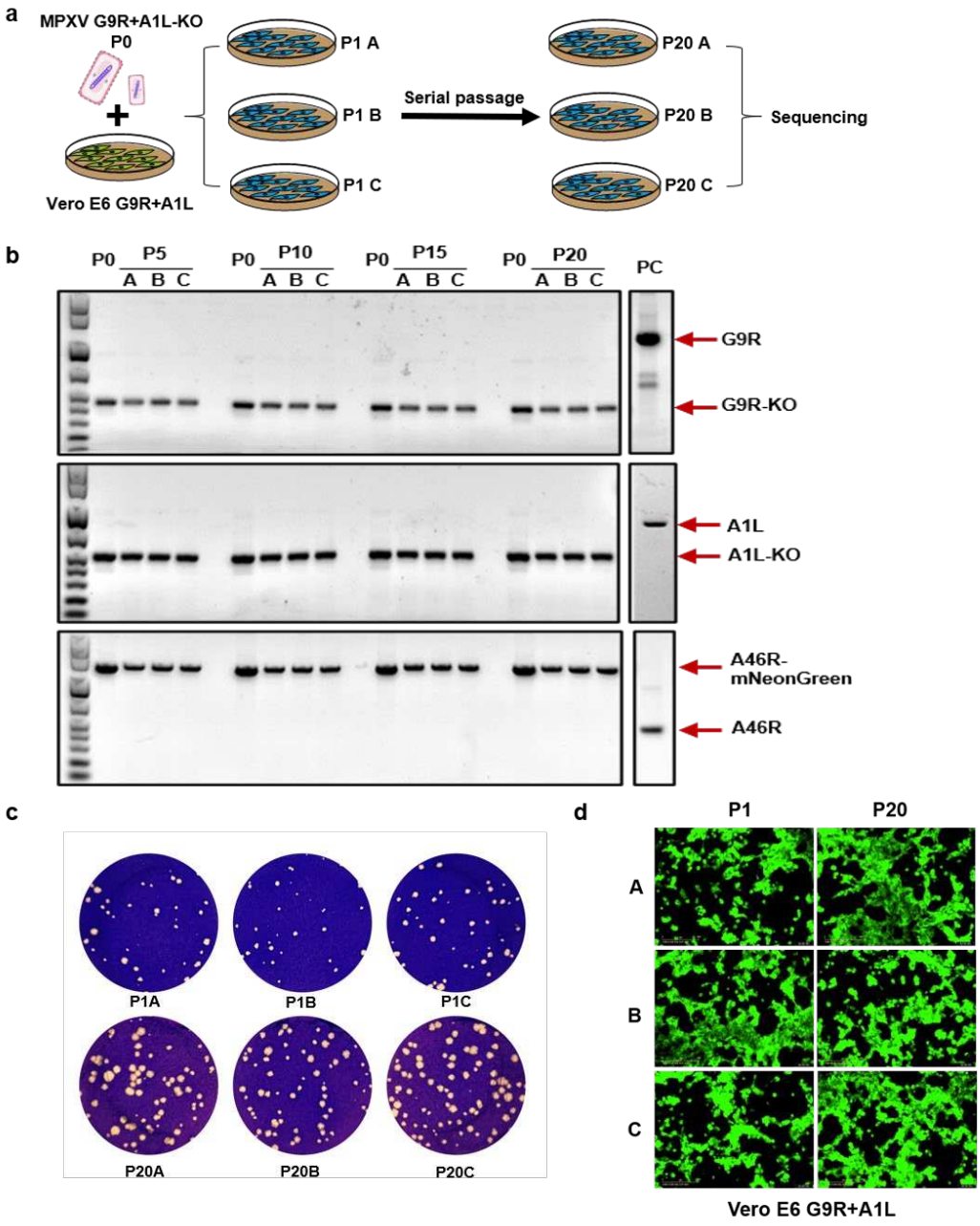

Extended Data Figure 3

Extended Data Figure 3. The serial passage of deficient MPXV in Vero E6 complementary cells.

a, Experimental scheme of serial passage of deficient MPXV in Vero E6 G9R+A1L cells. MPXV G9R+A1L-KO virion was continuously passaged on Vero E6 G9R+A1L cells for 20 rounds in 3 replicates. The full-length MPXV genome of P0 and P20 were subjected to sequencing. **b,** PCR confirmation of G9R and A1L gene deletions and mNeonGreen insertion in MPXVs across various passages. The samples were collected at passages 5, 10, 15, and 20, with P0 initial viruses serving as controls. **c,d** The plaque morphology (**c**) of fluorescence (**d**) comparison of deficient MPXV after serial passages. **c,** The plaques of MPXV G9R+A1L-KO virus at passage 1 and passage 20 in Vero E6 G9R+A1L cells were stained with crystal violet 6 days post-

696 infection. **d,** Vero E6 G9R+A1L cells were infected with P1 and P20 MPXV deficient
697 viruses at MOI of 0.1. Representative mNeonGreen positive images are shown 4 days
698 post-infection. Scale bar, 200 µm.

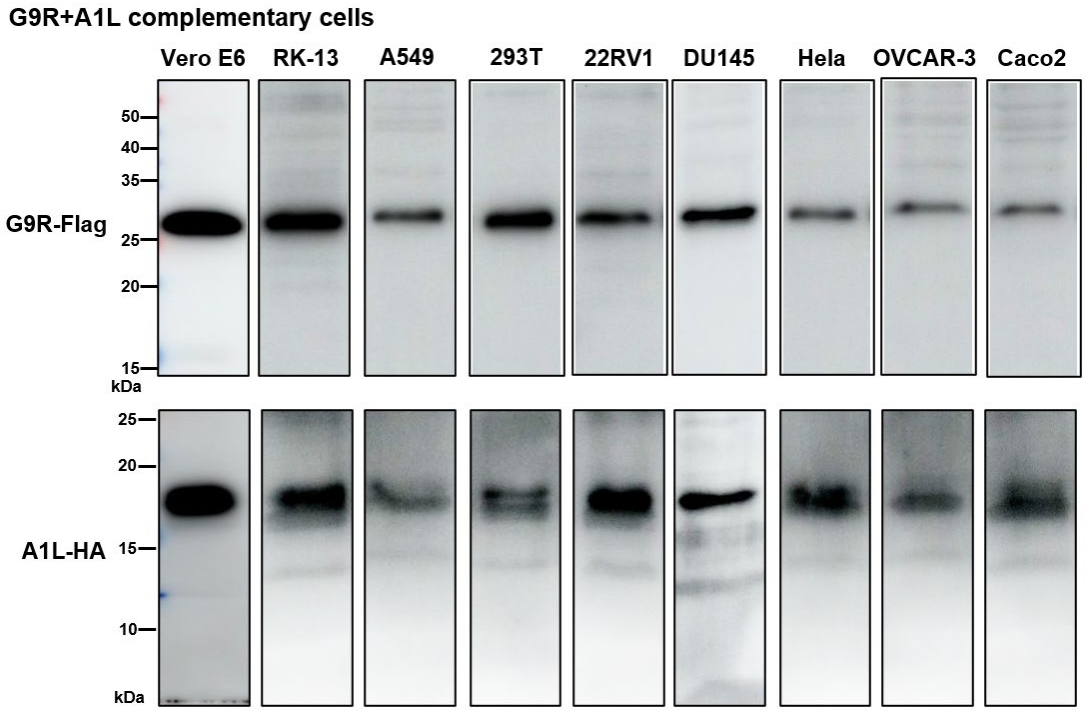

Extended Data Figure 4

Extended Data Figure 4. The expression of G9R and A1L genes in various complementary stable cell lines.

The expression of G9R and A1L genes in 9 G9R+A1L complementary cells were detected by western blot. The G9R and A1L proteins were respectively fused with flag or HA tags at the N-terminal of the proteins.

706 **Extended Data Table 1. The adaptive mutations of deficient MPXV after 20**
707 **passages.**

No.	Location	Region	Nucleotide	Amino acids	Replication
1	18318	D13L	C18318T	silent mutation	a
2	71481	G7R	C71481T	S32L	c
3	121858	Noncoding Region	^121859T	N/A	a
4	143761	A39R	T143761G	L79R	c
5	143739	A39R	Δ143739C	frame shift	b
6	145081	A40L	G145081T	Q113K	a
7	146786	A41L	G146786T	frame shift	c
8	146878-146922	Noncoding Region	Δ146878-146922	N/A	a, b, c
9	146999	A42R	Δ146999T	frame shift	a, b, c
10	170970	Noncoding Region	T170970G	N/A	a, b, c

708 The mutations in the noncoding and coding regions of MPXV G9R+A1L-KO between
709 passages P0 and P20 are noted. ^ symbol means insertion, Δ symbol means deletion.
710 a or b or c is biological replicate; N/A, Not Applicable.

711 **Extended Data Table 2. The IC_{50} values derived from plaque formation assay**
712 **and mNeonGreen positive cell counting assay.**

Drugs	Cells	IC_{50} uM (PFU)	IC_{50} uM (Fluorescence)
Tecovirimat	Vero E6 G9R+A1L	0.0038	0.002215
Cidofovir	Vero E6 G9R+A1L	6.776	1.239
Raltitrexed	A549 G9R+A1L	0.0823	0.2542
Tecovirimat	A549 G9R+A1L	0.0652	0.01138
Cidofovir	A549 G9R+A1L	48.29	12.83
Brequinar	A549 G9R+A1L	0.1236	0.4039
Buparvaquone	A549 G9R+A1L	3.854	5.956
Narasin	A549 G9R+A1L	0.0583	0.1294

713

714 **Extended Data Table 3. Primers used for construction of deficient MPXV.**

MPXV-F1	Forward primer	Reverse primer
F1a	GGAGTCACTAGTATTTAGGTGACACTATAGAAGGCG CGCCATACACCTGCAAAATGTGTGACCCACGACCGT AGGAAACT	AATAATCTATATGATTGGAGAAGTAGGAAACAAA CAGTAACAAGACGACG
F1b	ATCGTCGTCTTGTTACTGTTTGTTTCCTACTTCTCCA ATCATATAGATTATT	AATAATATAAGGATGATGAGAGGACGAGGATAGA TCGAAAAAAGCCACTA
F1c	ATTAGTGGCTTTTTTCGATCTATCCTCGTCCTCTCAT CATCCTTATATTATT	ATCGAATTCCATATCCGCGACTAAACAGTGAAAA ATGTAAATACTTTTTAAAT
F1d	TTTAAAAAGTATTTACATTTTTCACTGTTTAGTCGCGG ATATGGAATTCGATCCTG	TGTGCGGGTGTATAGAGTTCACAGTAGCTCATTC ACTTCTATTCAGTCAAAATG
F1e	TTTTGACTGAATAGAAGTGAATGAGCTACTGTGAACT CTATACACCCGCACAACTA	ATGAGTCCATGGATTAATATGAGTATAGTGTTAAA TGACACTTACTAAAAGCCAAA
F1f	GCTTTTAGTAAGTGTCATTTAACACTATACTCATATTA ATCCATGGACTCATAATC	GTATAAACTATCACGCGTTTGAATCGATATTAGAC TATATGCGCTGGAAGAAGATA
F1g	TTCTTCCAGCGCATATAGTCTAATATCGATTCAAACG CGTGATAGTTTATACCATT	TATTAATTTTTATACTATAATGGACAACACAACATT ATGTCGGTCGAGTATTATCT
F1h	AATACTCGACCGACATAATGTTGTGTTGTCCATTATA GTATAAAAATTAATATTTC	GTTAAGAGATGCATATGGATAGATATGTTGAATAT AGGGATAAACTTGTAGGGAAA
F1i	CCTACAAGTTTATCCCTATATTCAACATATCTATCCATA TGCATCTCTTAACACTC	TTTAAATTAATACGACTCACTATAGGGTCAGTGC GGCCGCCACCTGCTAATAGAATGCTAACGTAATA ATGCGTTATGAA
MPXV-F2	**Forward primer**	**Reverse primer**
F2a	GGAGTCACTAGTATTTAGGTGACACTATAGAAGGCG CGCCCACCTGCAGCATTCTATTATCCAGTGTTAAAAA AATTATC	TAACTGAAAAAAAAATTACTACTATTGTTAATTTAGT TATGGAACCTATCCTTGCAC
F2b	AAGGATAGGTTCCATAACTAAATTAACAATAGTAGTAA TTTTTTTTCAGTTATC	ACCTGGACTTTCGTTTGTAAATTGGGGCTTTTTG TACAATAAATGGGTGTTGCC
F2c	CAACACCCATTTATTGTACAAAAAGCCCCAATTTACA AACGAAAGTCCAGGTTTGAT	TAGAAAATAGAGACGTTATAGAACGCCATCATGT TAAACAGGATACAAACCTTGATG
F2d	AGGTTTGTATCCTGTTTAACATGATGGCGTTCTATAA CGTCTCTATTTTCTATTTT	TACAAAATGAGAATTCATTTATAGCATAGAAAAAA ACAAAATGAAATTCTACTATA
F2e	GTAGAATTTCATTTTGTTTTTTTCTATGCTATAAATGAA TTCTCATTTTGTATCCGC	ACAAATTTTAGTACTATTAACGCGACTAGTATTCT CTAAAGATGATATCTGT
F2f	ACAGATATCATCTTTAGAGAATACTAGTCGCGTTAATA GTACTAAAATTTGTAT	ATATACAAATTATTAATAATATATTTGGTTTGTTCTA TGATCTACCGTGCCTTATC
F2g	AGGCACGGTAGATCATAGAACAAACCAAATATATTAT TAATAATTTGTATATACAT	TTTAAATGAAAATATATTTCTAAATTCTAGAAATGG ATGTTAGGTGTATTAATTGG
F2h	TTAATACACCTAACATCCATTTCTAGAATTTAGAAATAT ATTTTCATTTAAATGAATC	TTTAAATTAATACGACTCACTATAGGGTCAGTGC GGCCGCCACCTGCTATAGCGTTTGTCTTCTGTA GTTGGTTATCATA
MPXV-F3-G9R-KO-mCherry	**Forward primer**	**Reverse primer**
F3a	GGAGTCACTAGTATTTAGGTGACACTATAGAAGGCG CGCCCACCTGCACAAACGCTATAAAAAACATAATTAC GACGAGC	TAAATAATTTTTTTTATTACACCAACAAAAATGTTT GTCATTAAACGAAATGGATA
F3b	CATTTCGTTTAATGACAAACATTTTTGTTGGTGTAATA AAAAAAATTATTTAATTTTTCA	AAAAGATGTGGTCATTAGATTTTGATTTTTAGTTA TTATCTACAGGAACAAATATAGTAT
F3c	TTTGTTCCTGTAGATAATAACTAAAAATCAAAATCTAA TGACCACATCTTTTTTTAGA	ACGATTTTAAGTTTTTGATACCCATAAATGAAGAA CGTACTGATTATTTTCGGTAAAC
F3d-G9R-KO-mCherry	CGAAAATAATCAGTACGTTCTTCATTTATGGGTATCAA AAACTTAAAATCGTTACT	ACTTACTCCGCCACCCATATTTATCTCATTGAAA GTATTAGTCTAAAAACGCCATA
F3e	GCGTTTTTAGACTAATACTTTCAATGAGATAAATATGG GTGGCGGAGTAAGTGTTG	TACATTAGGAACATTCTCCATTTATAGTAATCAAT CCTTTGTCGGAATATCTGTTA
F3f	AGATATTCCGACAAAGGATTGATTACTATAAATGGAG AATGTTCCTAATGTATACT	GAGATTACAGCCATTTTTATCAAGTCAGTTTCTTT TAAAGAACCGAAGGTATACAA
F3g	ATACCTTCGGTTCTTTAAAAGAAACTGACTTGATAAA AATGGCTGTAATCTCTAAG	TTTAAATTAATACGACTCACTATAGGGTCAGTGC GGCCGCCACCTGCTCTAACACTTATTCCATATTA CTAAGATCGGAA
MPXV-F4-A1L-KO	**Forward primer**	**Reverse primer**
F4a	GGAGTCACTAGTATTTAGGTGACACTATAGAAGGCG CGCCCACCTGCATAAGTGTTAGATAAATGCGGTAAC AAATGTTC	TTCGTAATTGACCACGCCATTACGATACAAACTT AACGGATATCGCGATAATGAAA
F4b	ATTATCGCGATATCCGTTAAGTTTGTATCGTAATGGC GTGGTCAATTACGAATAAAGC	ATGATACTATGTTGGCATCCATATTGTGTTTTATTA TAAACGACTAGTTTTTTTTC

F4c	AAAAACTAGTCGTTTATAATAAAACACAATATGGATGC CAACATAGTATCATCTT	ATAGCCGCATCCATTTAGAACACAAGTTAAAATTT CACTAAAGCATTAATAAATAA
F4d	TTATTAATGCTTTAGTGAAATTTTAACTTGTGTTCTAA ATGGATGCGGCTATTAGAGG	ACAAAGCTCGACATTTATTTCTTTATATATCTCATC AGTTTTATGGAGAAGATACCAC
F4e	TCTTCTCCATAAAACTGATGAGATATATAAAGAAATAA ATGTCGAGCTTTGTTACC	TTTTTAAAACATAGTTATTACTTATCACTCATAAAT GAGTAAATCACACGCGGCCT
F4f-A1L-KO	CGCGTGTGATTTACTCATTTATGAGTGATAAGTAATAA CTATGTTTTAAAAATCAC	CTTGTTCATTAGAAGTATAAAAGACGGTGTTTAC GGAAGCT
F4g	AGCTTCCGTAAACACCGTCTTTTATACTTCTAATGAA CAAG	TAATAAGATTGGATATTAAAATCACGCTTTCGAGT AAAAACTACGAATATAAATAA
F4h	TTATATTCGTAGTTTTTACTCGAAAGCGTGATTTTAAT ATCCAATCTTATTACTTTTG	TTTAAATTAATACGACTCACTATAGGGTCAGTGC GGCCGCCACCTGCTAAATCTGTAAATAAATAATG GACAAACTTAGA
MPXV-F5	**Forward primer**	**Reverse primer**
F5a	GGAGTCACTAGTATTTAGGTGACACTATAGAAGGCG CGCCCACCTGCTTTACAGATTTAGTTGTTTAATTTATT TGTGCT	TGACTCTGTCTCTTTTGATGATGAATAAATGTCAT GTTATACAGCTATATTAAAATC
F5b	TAATATAGCTGTATAACATGACATTTATTCATCATCAAA AGAGACAGAGTCACCAT	TTGTCTGGATATGGGAATGTATTAAATTAAATAATT TTAATTCGTTTAACGAATATCT
F5c	TCGTTAAACGAATTAAAATTATTTAATTTAATACATTCC CATATCCAGACAACAATCG	ATACTCCATCTTTAATAGTGACATTTTTTAATATAT AAATGAGTTATTTAAGATAT
F5d	CTTAAATAACTCATTTATATATTAAAAAATGTCACTATT AAAGATGGAGTATAATCT	TTTAAAATAGTCGAAATGGCGTTACTAACGTTATT ACATTTTTTTTATGTAATTTCT
F5e	TTACATAAAAAAAATGTAATAACGTTAGTAACGCCATT ATGGATAATCTATTTACCTT	AGTGAATTAGCTTATCTTGATGAGTATCTACTAAA CAATATTATACCAGAAAAGACG
F5f	TTTCTGGTATAATATTGTTTAGTAGATACTCATCAAGA TAAGCTAATTCACTAAACAT	GGGAGATCTACGATCTTATAATTACCCGATTGTA GTTAAGTTTTGAATAAAAATTT
F5g	TTTTATTCAAAACTTAACTACAATCGGGTAATTATAAG ATCGTAGATCTCCCATGT	CCTAAGTGTATTTAAAATAGATGTCATGTTAAAAA TGTCAGCTGCCGACTTTTTGGAA
F5h	AAAGTCGGCAGCTGACATTTTTAACATGACATCTATT TTAAATACACTTAGGTTTT	TTTAAATTAATACGACTCACTATAGGGTCAGTGC GGCCGCCACCTGCACGTTAACGACTTACTATTAA TTCATTTTTTGT
MPXV-F6-A46R-mNG	**Forward primer**	**Reverse primer**
F6a	GGAGTCACTAGTATTTAGGTGACACTATAGAAGGCG CGCCCACCTGCAGTCGTTAACGTACGCCGCCATGG ACGCCGCGT	AAGAAAAAAATTGATAATTGTTAATTGTTATTTTTA TACAACAAAACGGTACGGTG
F6b	GTACCGTTTTGTTGTATAAAAATAACAATTAACAATTAT CAATTTTTTTCTTTAATAT	CTTCTCCTTTGCTCACCATTATTTAGTAAAATAGA AT
F6c-mNeonGreen-F2A-A46R	ATTCTATTTTACTAAATAATGGTGAGCAAAGGAGAAG	CTCGACGTCTCCCGCCAGCTTGAGAAGGTCAA AATTCAACAGCTGCTTGTAGAGTTCGTCCATT
	GACCTTCTCAAGCTGGCGGGAGACGTCGAGTCCAA CCCTGGGCCAATGGCTGTTTGTATAATAG	ACGTATCACTTGTTTAATATCTATATCAGCTATTCT GGAACCGAGTACTTCCACAT
F6d	GGAAGTACTCGGTTCCAGAATAGCTGATATAGATATT AAACAAGTGATACGTAAGA	AAAAAAATAACAAATATGGAATACAACCTTATATAT TTTTGCTCTCATTAACTTTT
F6e	GTTAATGAGAGCAAAAATATATAAGGTTGTATTCCATA TTTGTTATTTTTTTCTGT	CCTCTCAATATGATAGATTTTATTATCCCAGATATT TATGTAAGTCAAAAATCTAG
F6f	ATTTTTGACTTACATAAATATCTGGGATAATAAAATCTA TCATATTGAGAGGACCA	TATATAATTTATATTCTGTAACATGTTATCCCTTTTC AATGAACAGTGTTAGTTTA
F6g	CTAACACTGTTCATTGAAAAGGGATAACATGTTACAG AATATAAATTATATATGGA	CATGGTGTTGTTTGTTATTTGACTACTGTCACTG AAGTGATAATATATTTTAAATTTT
F6h	TAAAATATATTATCACTTCAGTGACAGTAGTCAAATAA CAAACAACACCATGAGAT	TTTAAATTAATACGACTCACTATAGGGTCAGTGC GGCCGCATTGGTCGTGTAGCGCGATAGAGATAG TCTAATAT
MPXV-F7	**Forward primer**	**Reverse primer**
F7a	GGAGTCACTAGTATTTAGGTGACACTATAGAAGGCG CGCCCACCTGCACACGACCAATATCGATTACTATGG ATATCTTC	TCTTCATCTTCATCTTCATCTTCATCATAGGTACT AAGATAATTATATAATATCAGTT
F7b	TATTATATAATTATCTTAGTACCTATGATGAAGATGAAG ATGAAGATGAAGATGATGG	TAACATCTTCTACTTATCATCACCCATTGTATAAC ATTCTATAGTTCGTTTTACGTTC（
F7c	AAAACGAACTATAGAATGTTATACAATGGGTGATGAT AAGTAGAAGATGTTACCCGAT	TCCAAAAATCCTATATTACCATGTAATGTGTTATT GTTAGATGTCTCATCATCAAC
F7d	ATGATGAGACATCTAACAATAACACATTACATGGTAAT ATAGGATTTTTGGAAATAAA	TATGTCCGTTTCTTAGTTTTAGCATCTTCCCAAAA TGAATTAGGGTTGTCATATCCAT
F7e	ATGACAACCCTAATTCATTTTGGGAAGATGCTAAAAC TAAGAAACGGACATATAGTGC	TCTTAGAAATGCCATTCGTATGTACACGCTGGCA GACGCCACCGAGCTGTCATAGT

F7f	TGACAGCTCGGTGGCGTCTGCCAGCGTGTACATAC GAATGGCATTTCTAAGAAAAG	GGCTTTTTTCGATCTATCAATTTCAGTATATTCGT CGCCGTTATAAAAGTAATGTTGT
F7g	TTACTTTTATAACGGCGACGAATATACTGAAATTGATA GATCGAAAAAAGCCACTAAT	CTATCTTATCGAATGATATATTTTTCATAAATACAC TTTTATAGTCCTCGTTTAAACA
F7h	AAAAGTGTATTTATGAAAAATATATCATTCGATAAGATA GATTCCATCATCGAAAAAT	TTTAAATTAATACGACTCACTATAGGGTCAGTGC GGCCGCATACACCTGCAAAATGTGTGACCCACG ACCGTAGGAAACT

715